Optica Applicata, Vol. XXXVII, No. 3, 2007

Web camera-enabled material research: an acoustooptic example

G. ALEXIEVA, I. TRAYKOV, V. STRASHILOV*

Sofia University, Faculty of Physics, Department of Solid State Physics and Microelectronics, 5 J. Bourchier Blvd., 1164 Sofia, Bulgaria

*Corresponding author: ves@phys.uni-sofia.bg

The applicability of standard PC web cameras to material testing has been discussed. A simple method for measuring the acoustic velocity and attenuation of transparent solid materials has been described as an illustrative example. It is based on the acoustooptic diffraction in the Raman–Nath limit and a digital readout and processing of the information obtained. Acceptable accuracy of the results is achieved. The method is particularly suitable for very quick testing of high loss materials.

Keywords: web camera, acoustooptic diffraction, material testing, acoustic velocity and attenuation.

1. Introduction

Material research methods often employ light as a probing tool to reveal macroscopic or microscopic properties. In various applications, the spatial distribution of the emitted or scattered light intensity is mapped electronically to obtain a desired feature. This trend has been pushed forward in recent decades by the advent of the optical detection matrices (or image sensors). The advantage offered by these matrices is basically twofold: *i*) they spare the effort required in older systems to displace individual diode detectors across the area under study; *ii*) when digitized, they are readily connectable to personal computers to perform on-line numerical processing of the data obtained.

The available numerous types of optical matrices, their operational regimes and measurement capabilities hardly need to be discussed in a contribution like this. We restrict ourselves here to the web cameras and by this term we mean the least expensive charge-coupled device (CCD) or complementary metal-oxide semiconductor (CMOS) cameras that are typically used as inherent parts of computers. We do not mean the much more expensive cooled CCD cameras whose performance is expectedly (but not necessarily) higher. What we consider as most important in this discussion is the fact that, with contemporary computing means, quite modest types of devices are

sometimes capable of delivering information that is adequate enough to ensure the receipt and processing of optical experimental data.

A stimulus for this study came from a recent article posted on the Internet that compares the quality of astronomical pictures taken by web and cooled CCD cameras [1]. Surprisingly, the observations made by the web camera turn out to be of even higher quality, raising a number of questions concerning, for example, the role of timing (sampling and image rates) in measuring unstable patterns. Other research applications of the web camera could be found in areas so much different as watermark detection [2] and robotics [3]. The present study illustrates its potential in classical optical research of transparent materials, specifically addressing the acoustooptic diffraction method.

2. Material properties studied by acoustooptic diffraction

The acoustooptic interaction has proved to be a powerful means for studying sound waves in transparent solids and liquids [4]. Although different aspects of this interaction have been known, the acoustooptic diffraction has occupied the major place in both research and applications. Depending on a number of parameters, mainly the acoustic frequency and the aperture of the sound beam within the solid sample, the diffraction displays two limit regimes: the Raman–Nath limit with a multitude of diffraction orders, and the Bragg limit with only one pronounced order. The Bragg diffraction is much more efficient but at the same time more difficult to realize because of the restrictive angular rules.

There are two integral acoustic parameters – the acoustic wave velocity and attenuation – that are directly related to the diffraction output. The attenuation affects the intensity of the diffracted light via the acoustic power flow in the sample at the cross point with the incident light beam. To measure the attenuation, either the light beam or the illuminated sample has to be shifted along the acoustic propagation path to monitor the decay of power [5, 6]. The velocity, on the other hand, determines the angular separation of the diffracted orders. Its measurement requires finding the position of an order with respect to that of the zeroth order in a plane normal to the acoustic wave vector [6]. Apart from this geometrical role, the velocity has a critical impact on the efficiency of the diffraction, reducing the diffracted intensity proportionally to its third power [7].

The propagation of an acoustic wave in a solid medium is accompanied by effective interaction of the acoustic phonons with defects and various elementary excitations such as thermal phonons, free electrons, excitons, *etc*. Thus, the obtained velocity and attenuation might provide information about the microscopic status of the material under investigation, the characteristics of its elementary excitations or, in general, its scope of applicability as acoustic material. A typical example is a recent acoustooptic study of the relaxation of the ionic motion in photochromic glasses [8].

In most acoustooptic studies the diffracted light has been captured by sensitive detectors, such as photo-multipliers or diodes, to monitor the position and intensity of order spots. The measurements require goniometry, cumbersome electronics and extensive analog information processing. The advent of the optical matrix detectors has provided the option of a simple digital readout of the diffracted intensity distribution. Similar procedures have recently been followed in a number of studies, concerning, for example, the surface profiling of thin films [9] or the ultrasound modulated optical tomography of living subjects [10].

3. A digital acoustooptic scheme for measuring sound velocity and attenuation

The experimental acoustooptic setup for the present study is illustrated in Fig. 1. The light beam from a 1 mW semiconductor laser with $\lambda = 635$ nm is directed at normal incidence to one of the sides of a parallelepiped sample made from the transparent solid material under study. The sample is placed in a holder mounted on a three-dimensionally moving bench with a step of 10 μm along each direction. The light interacts with a longitudinal acoustic wave continuously generated in the sample by a ceramic transducer of fundamental frequency 7.6 MHz, fed from a digital PC generator (ETC-M631) connected to the printer port of a computer (Pentium IV, 3 GHz, 1 GB RAM). Owing to the right angle between the two wave vectors and a relatively low frequency, the resulting diffraction of light is dominated by the Raman–Nath limit. The diffracted light is passed consecutively through an attenuating filter and a focusing lens, so that the first few diffracted orders of + and – directivity are sensed by the open active area of a standard web camera (QuickCam Logitech, 640×480 pixels, 7.5 μm per pixel, 30 frames per second). The output of the camera is fed to the USB port of the computer for image reconstruction and

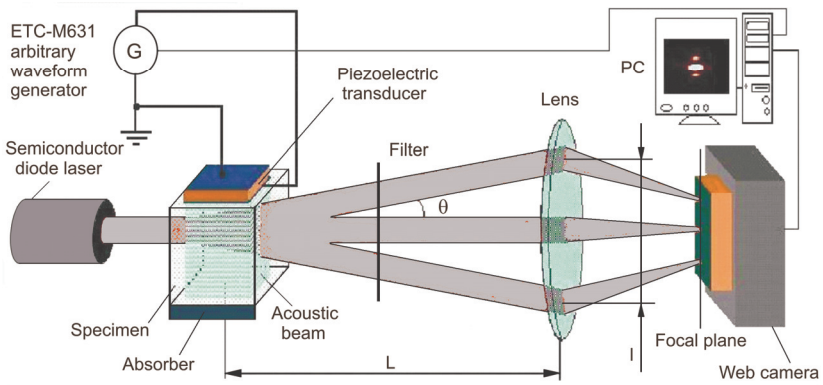

Fig. 1. Experimental setup for acoustooptic diffraction studies using web camera as light detector.

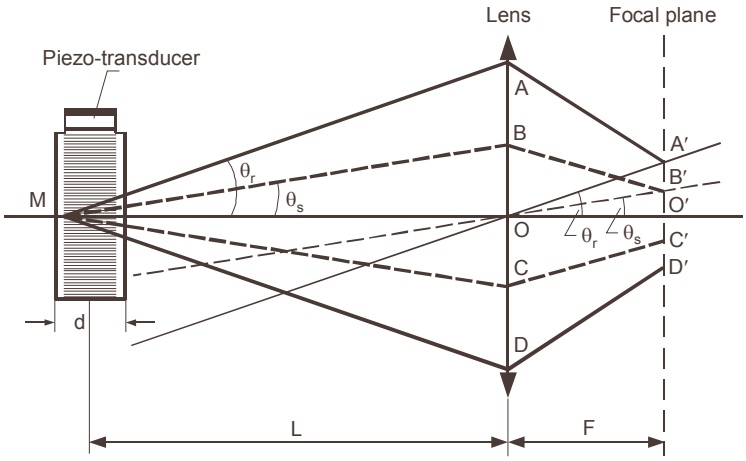

Fig. 2. Two diffraction orders at angles θ_r and θ_s resulting from diffraction from reference sample and the sample under study.

processing of the data via Matlab. As the diffracted pattern seen by the camera is a size-contracted replica of the real pattern, it is possible to obtain an absolute estimate of the real order spacing. However, this approach requires, as in all classic studies, that the distance L between the sample and the lens be precisely known (Fig. 2), which complicates the experiment. We adhere to a different approach where this requirement is removed by comparing the pattern generated by the sample being studied to that from a reference sample with known acoustic velocity.

The acoustic velocity V can be deduced from the angular condition for the first Raman–Nath diffraction order [7]:

$$\sin\theta_0 = \frac{\Lambda}{\lambda n} = \frac{\Lambda f}{Vn} \tag{1}$$

where θ_0 is the diffraction angle in the sample, Λ – the light wavelength in vacuum, λ – the acoustic wavelength, f – the acoustic frequency and n – the refractive index of the sample. The angle θ which we measure in air is larger because of the refraction at the sample/air interface. In the general case, it involves a combination of the distance L, the sample width parallel to the propagation direction d, and the refractive index n, which ultimately makes the proposed comparative approach inapplicable. However, the simplifying condition of large L compared to d reduces this formula to:

$$\sin\theta \approx \frac{l}{2L} = \frac{\Lambda}{\lambda} = \frac{\Lambda f}{V} \tag{2}$$

Here, l denotes the spacing between the +1st and –1st diffraction orders; it should be measured upon screening out the zeroth order to reduce the noise.

Let us define two angles θ_s and θ_r corresponding to diffraction caused the sample under study and a reference sample, respectively. This sub-index convention holds for all quantities to be used in further calculations. In order to ensure equivalence in the experimental conditions, the two samples are provided with identical transducers, generating along parallel lines. The samples are placed side by side in the holder, so that the light can just be switched from one sample to the other at unchanged positions of the laser and the web camera. The two characteristic spacings l_s = AD and l_r = BC are projected on the focal plane as l'_s = A'D' and l'_r = B'C', see Fig. 2. The similarity of triangles indicates that:

$$\frac{l_s}{l_r} = \frac{l'_s}{l'_r} \tag{3}$$

From (2) and (3) it readily follows that:

$$V_s = \frac{l_r f_s}{l_s f_r} V_r = \frac{l'_r f_s}{l'_s f_r} V_r \tag{4}$$

To measure the acoustic attenuation the sample should be shifted parallel to the acoustic wave vector and the intensity of one of the diffraction orders should be measured as a function of distance X. Matlab permits digitization of the detected image pattern into 256 shades of gray that is quite a satisfactory resolution for the pixel intensity. The spatial intensity variation obtained is then exponential-fitted to give the attenuation:

$$I_d = I_{d_0} \exp(-\alpha_l x) \tag{5}$$

A well-established fact for the Raman–Nath diffraction limit is the linearity between the diffracted light intensity and the acoustic power P at non-elevated power levels [4]. Thus the optical intensity decay α_l is just the acoustic power attenuation, *i.e.*, twice the acoustic amplitude attenuation:

$$\alpha_l = 2\alpha_a \tag{6}$$

Apart from simplicity and computer-aided performance, this method has another major advantage over conventional pulse-echo and interference methods [11]. It is applicable to high loss materials that do not tolerate multiple echoes. With such materials even the detection of the first echo might be problematic. However, illuminating the near-field region close to the transducer should, in principle, provide a detectable diffraction regardless of the magnitude of attenuation. The accuracy of the velocity measurement depends on the error in measuring the order spacings and the reference velocity, and is typically of the order of a few percent. The accuracy of

the attenuation cannot be specified in rigorous terms because of the factors influencing the detection during the movement of the sample at long continuous exposures of the web camera. More details will be provided in the next section.

4. Experimental results and concluding remarks

Two experimental samples have been prepared in the form of parallelepipeds with optically flat sides. They are made of isotropic materials to avoid any side effects, such as beam steering, which could violate the experimental equivalence. The reference sample is of vitreous silica glass doped with lead inclusions to reduce the acoustic velocity and thus improve the diffraction efficiency. Its longitudinal velocity has been measured by a pulse-echo method: $V_r = 3935$ ms^{-1} ± 0.8%. The sample is made of polymethilmetacrylate (PMMA). The small bases of the parallelepipeds are provided with ceramic PzT transducers firmly attached by epoxy bond. As neither of the transducers is matched to its load, the frequency of operation should be adjusted to reach maximum power within the available frequency band. Therefore, the two frequencies involved in Eq. (4) are generally different. The holder carrying the two samples is located at distance $L = 70$ cm from the focusing lens (focal length $F = 10$ cm), much larger than the samples' width d that is of the order of a few milimeters. Under these geometrical conditions and the operating frequency range used, the real order spacing is of the order of a few milimeters; this is contracted by the lens to hundreds of micrometers (tens of pixels) on the camera sensor plane. All experiments have been carried out at room temperature and have been compared to room temperature data from literature.

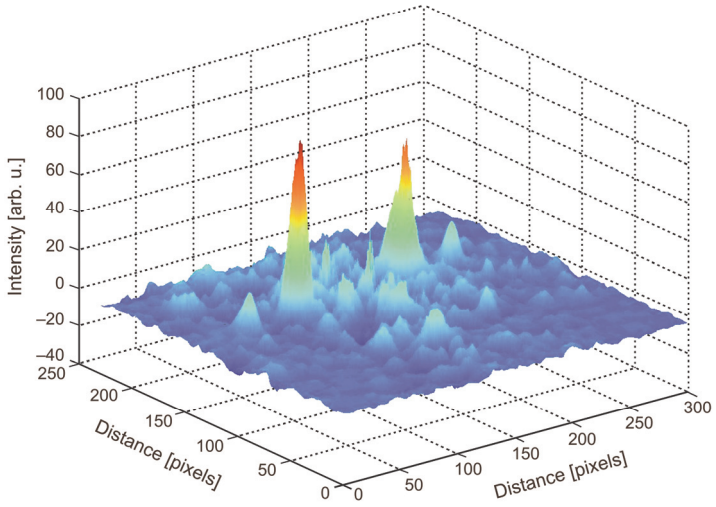

Fig. 3. Plane distribution of the light intensity diffracted from the PMMA sample at 7.8 MHz.

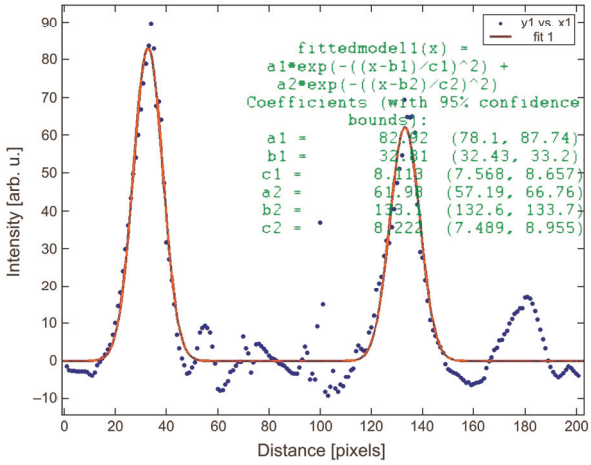

Fig. 4. Cross-section of the intensity surface from Fig. 3 and Gaussian fit of the envelope function.

The experimentally registered diffraction caused the PMMA sample is illustrated in Figs. 3 and 4. Figure 3 is a view of the plane distribution of the diffracted intensity involving the first four Raman–Nath orders: ±1st and ±2nd (weakly expressed). The operating frequency is 7.8 MHz. In this figure, the strongly dominating background intensity of the incident laser beam (zeroth order) has been mathematically removed to clearly reveal the ±1st orders and make further calculations easier. This is done by subtracting the intensity distribution measured without sound excitation from the full diffraction picture. In Figure 4, a cross-section of the intensity surface with a vertical plane passing through the positions of the two maxima is presented. The resulting dependence is given a Gaussian fit to determine the characteristic spacing $l'_r = 100.3$ pixels. Similarly, the corresponding order spacing in the silica case is $l'_s = 79.3$ pixels at 9.2 MHz (not shown). Following Eq. (4), the resulting longitudinal velocity of PMMA is $V_s = 2630$ ms^{-1} ± 3.2%. Besides the 0.8% tolerance for the reference velocity, the overall error of the result involves 1% for each of the two order spacings as following from the corresponding Gaussian confidence intervals. Another 0.4% comes from neglecting the finite width of the sample, while the acoustic frequency, measured to around 100 Hz, practically does not affect the accuracy. The mean velocity value obtained is very close to that measured by high-frequency time-resolved broad-band microscopy (2640 ± 4 ms^{-1}) [12]. However, it deviates significantly from higher values measured by pulse-echo techniques in [13, 14], which even fall out of our confidence interval. This inconsistency is another clear indication that polymer acoustic constants should be treated with much care concerning the experimental method and its inaccuracy. It is possible that some deviations might also be due to differences in the conditions of material polymerization.

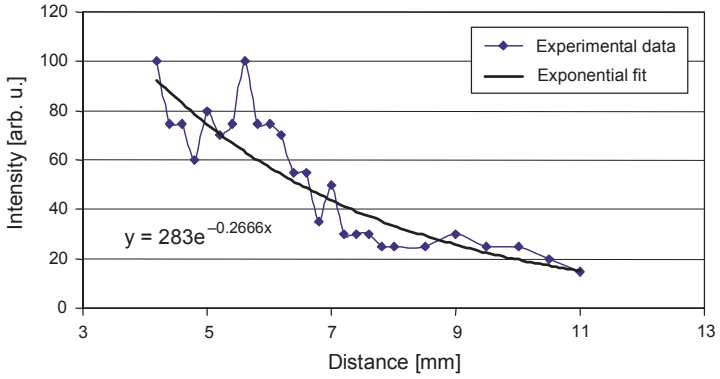

Fig. 5. Diffracted intensity versus distance in the PMMA sample.

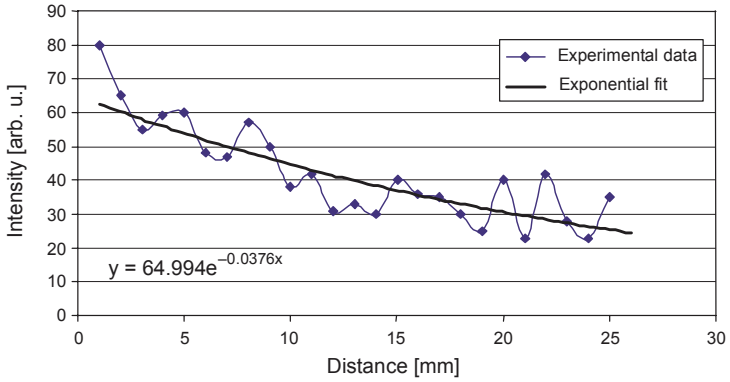

Fig. 6. Diffracted intensity versus distance in silica glass sample at 9.2 MHz.

The measurement results for the acoustic attenuation are shown in Fig. 5 (PMMA) and Fig. 6 (silica), respectively. During the experiments the sample is moved with a step of 1 mm and the evolution of a specified order is monitored at a constant position of the web camera. At each sample position the diffracted intensity is determined as the amplitude of the Gaussian function and the resulting sequence of peak intensity values is fitted exponentially to give the attenuation. The calculated value for the attenuation in PMMA is 133 Np m^{-1}. It should be compared to 106 Np m^{-1} measured under similar conditions (room temperature and 10 MHz) in [14]. The value obtained for silica is 19 Np m^{-1} (1.3 Np m^{-1} for pure silica [15]). There is no reason for making a comparison with literature data in the latter case because the attenuation of these glasses is heavily dependent on the lead content and the preparation mode. As commented in the previous section, it is not possible to provide a rigorous analysis of the accuracy of the attenuation result. This is manly due to fluctuations of the camera output, which limit the confidence of the exponential fitting. A plot of the time

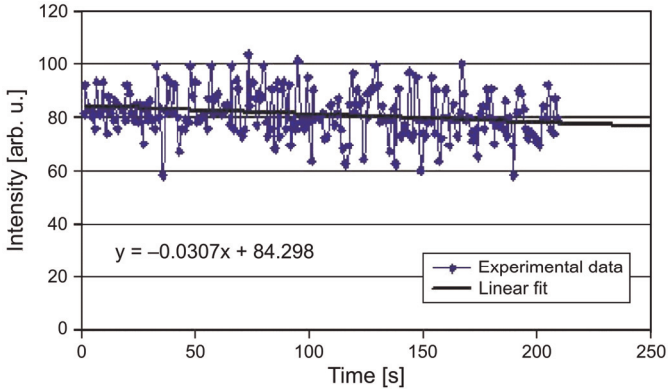

Fig. 7. Short term stability of the web camera output at a constant position of the sample.

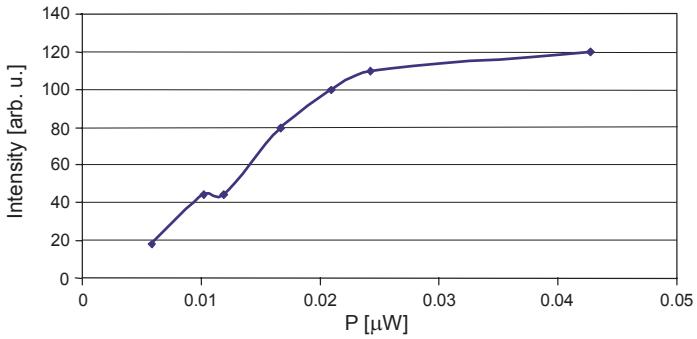

Fig. 8. Measured intensity versus incident optical power as a measure of camera linearity.

dependence of the signal at a constant position of the sample is shown in Fig. 7. Apart from the considerable noise, there is a tendency towards casual floating of the average level that affects the attenuation estimate at longer exposures of the camera. The value and even sign of this instability arise from semiconductor surface state statistics at ambient temperatures and are difficult to predict. Another source of errors might be a departure from linearity of the camera response. However, as is evident from the measured characteristics of Fig. 8, this departure occurs above the working range of this study (0–100 arb. units). A rough estimate of the overall accuracy of the attenuation might be a 30% deviation from literature data in the PMMA case. In view of the simplicity and rapidity of the method the featured accuracies of velocity and attenuation might be considered as acceptable. The method is particularly applicable to very quick testing of the acoustic properties of transparent lossy materials.

Acknowledgments – This work has been partially supported by the Scientific Fund of Sofia University under grant No. 004/2007.

References

[1] LEGAULT T., www.astrophoto.fr/ccd_video.html.
[2] STACH J., BRUNDAGE T., HANNIGAN B., BRADLEY B., KIRK T., BRUNK H., *Use of Web cameras for watermark detection*, Proceedings of the SPIE **4675**, 2002, pp. 611–20.
[3] KWON Y., RAUNIAR S., CHIOU R., SOSA H., *Remote control of quality using Ethernet vision and Web-enabled robotic system*, Concurrent Engineering Research and Applications **14**(1), 2006, pp. 35–42.
[4] STEGEMAN G.I., *Optical probing of surface waves and surface wave devices*, IEEE Transactions on Sonics and Ultrasonics **SU-23**(1), 1976, pp. 33–63.
[5] TUCKER J., RAMPTON V., *Microwave Ultrasonics in Solid State Physics*, North Holland 1972, Chapter 9.
[6] GUSEV O., KLUDZIN V., *Acoustooptical Measurements*, Edition of the University of Leningrad 1987, Chapter 1 (in Russian).
[7] DIEULESAINT E., ROYER D., *Ondes Elastiques dans les Solides: Application au Traitement du Signal*, Masson, Paris 1974; (*Elastic Waves in Solids: Application to Signal Processing*, Wiley, New York 1980), Chapter 8.
[8] KALININA A.S., PIROZERSKI A.L., CHARNAYA E.V., VASILIEV M.I., LEBEDEVA E.L., *Acoustooptic studies of ionic mobility in photochromic glasses*, Proceedings of the XVIII Session of the Russian Acoustical Society, 2006, pp. 22–5.
[9] AKIYAMA H., SASAKI O., SUZUKI T., *Sinusoidal wavelength-scanning interferometer using an acousto-optic tunable filter for measurement of thickness and surface profile of a thin film*, Optics Express **13**(25), 2005, pp. 10066–74.
[10] ZEMP R., KIM C., WANG L., *Ultrasound-modulated optical tomography with intense acoustic bursts*, Applied Optics **46**(10), 2007, pp. 1615–23.
[11] ELBAUM R., CHICK B., *Ultrasonic Methods in Solid State Physics*, Academic 1969, Chapter 2.
[12] RAUM K, BRANDT J., *Simultaneous determination of acoustic impedance, longitudinal and lateral wave velocities for the characterization of the elastic microstructure of cortical bone*, Proceedings of the World Congress on Ultrasonics 2003, Paris 2003, pp. 321–4.
[13] AZZALI M., RUGGINI C., TIZZI R., *Investigation on the ability of Tursiops truncatus to discriminate, recognise and classify geometric shapes using visual and/or acoustic perception*, Proceedings of the 13th Annual Conference of the European Cetacean Society, 1999, pp. 51–9.
[14] CARLSON J., VAN DEVENTER J., SCOLAN A., CARLANDER C., *Frequency and temperature dependence of acoustic properties of polymers used in pulse-echo systems*, 2003 IEEE Ultrasonics Symposium, pp. 885–8 .
[15] MASON W., MCSKIMIN H., *Attenuation and scattering of high frequency sound waves in metals and glasses*, Journal of the Acoustical Society of America **19**(3), 1947, pp. 464–73.

Received May 15, 2007
in revised form July 31, 2007